High-Contrast Qubit Interactions Using Multimode Cavity QED

David C. McKay,[1,*] Ravi Naik,[1] Philip Reinhold,[1,†] Lev S. Bishop,[2,3] and David I. Schuster[1]
[1]James Franck Institute and Department of Physics, University of Chicago, Chicago, Illinois 60637, USA
[2]Condensed Matter Theory Center, Department of Physics, University of Maryland, College Park, Maryland 20742, USA
[3]IBM T.J. Watson Research Center, Yorktown Heights, New York 10598, USA
(Received 7 May 2014; revised manuscript received 22 October 2014; published 27 February 2015)

We introduce a new multimode cavity QED architecture for superconducting circuits that can be used to implement photonic memories, more efficient Purcell filters, and quantum simulations of photonic materials. We show that qubit interactions mediated by multimode cavities can have exponentially improved contrast for two qubit gates without sacrificing gate speed. Using two qubits coupled via a three-mode cavity system we spectroscopically observe multimode strong couplings up to 102 MHz and demonstrate suppressed interactions off resonance of 10 kHz when the qubits are ≈600 MHz detuned from the cavity resonance. We study Landau-Zener transitions in our multimode systems and demonstrate quasiadiabatic loading of single photons into the multimode cavity in 25 ns. We introduce an adiabatic gate protocol to realize a controlled-Z gate between the qubits in 95 ns and create a Bell state with 94.7% fidelity. This corresponds to an on/off ratio (gate contrast) of 1000.

DOI: 10.1103/PhysRevLett.114.080501 PACS numbers: 03.67.Lx, 42.50.Pq, 84.30.Vn, 85.25.-j

Circuit cavity quantum electrodynamics (cQED) using superconducting resonators and Josephson junction based qubits has demonstrated the essential building blocks of gate based quantum computing and quantum optics [1]. Typically, cQED devices are engineered so that the qubits primarily couple to a single cavity mode; nonetheless, the true multimode nature of these devices is unavoidable. For example, a multimode treatment is required to correctly understand the Purcell effect [2], and to model the device parameters for qubits coupled to 3D resonators [3]. Although these modes are usually treated as a nuisance, if properly utilized, they are a powerful asset. In this Letter, we introduce an explicitly multimode QED architecture as a resource to study multimode quantum optics [4], as a many-body bosonic system for quantum simulation [5,6], as a photonic register for quantum memory [7], to filter the noise environment [8,9], and to tailor coherent qubit-qubit interactions.

In the context of quantum computing, tailoring qubit interactions is of paramount importance for improving gate contrast. In the past several years much effort has been spent to improve gate fidelities and coherence times [10–12], leading to rapid progress towards constructing larger circuits [12–16]. However, as strongly coupled circuits grow larger, issues inevitably arise due to residual cQED couplings. Several methods have been developed to reduce unwanted interactions; however, they are not without their limitations. The most common approach is to develop tunable interactions by coupling through a resonant interaction and controlling the detuning from resonance, imposing a tradeoff between gate contrast and speed. In this approach, expanding beyond two qubits results in spectral crowding, which limits addressability [17] and introduces spurious avoided crossings. Alternatively, we can directly tune the coupling parameters [18–21]; however, these additional tunable elements introduce complexity and a new path for decoherence.

In this Letter, we present a new multimode circuit QED architecture where qubits interact through a network of strongly coupled resonators, analogous to a multimode bandpass filter. The multimode architecture enables the off-resonant interactions to be suppressed exponentially in the number of modes (resonators) without any additional active elements. To demonstrate the multimode architecture, we construct a circuit with two transmon-type qubits coupled via a three-mode (three-resonator) filter. We perform spectroscopy on our device and confirm the multimode circuit QED model. From spectroscopy, we observe multimode strong coupling when the qubit and filter are on resonance and suppressed qubit-qubit interactions when the qubit and filter are off resonance. Next, we measure strong interaction dynamics by quickly tuning the qubit energy into resonance with the filter. We demonstrate fast loading of single photons into the lowest mode of the filter (≈25 ns) and measure a single photon Stark shift greater than 100 MHz. Finally, we utilize the state-dependent Stark shift to realize a controlled-Z gate between the qubits in 95 ns and create a Bell state with 94.7% fidelity.

A schematic of our circuit and the corresponding physical realization are illustrated in Fig. 1. Three identical resonators of frequency ν_F are coupled to each other in a chain to form our multimode filter. Two flux-tunable transmon [22] qubits ($\nu_Q \approx 1$–9 GHz) are coupled to the resonators at the end of the filters. For qubit frequencies $\nu_{Q,1}, \nu_{Q,2}$, the qubit-filter system (for n modes) is described by the Hamiltonian

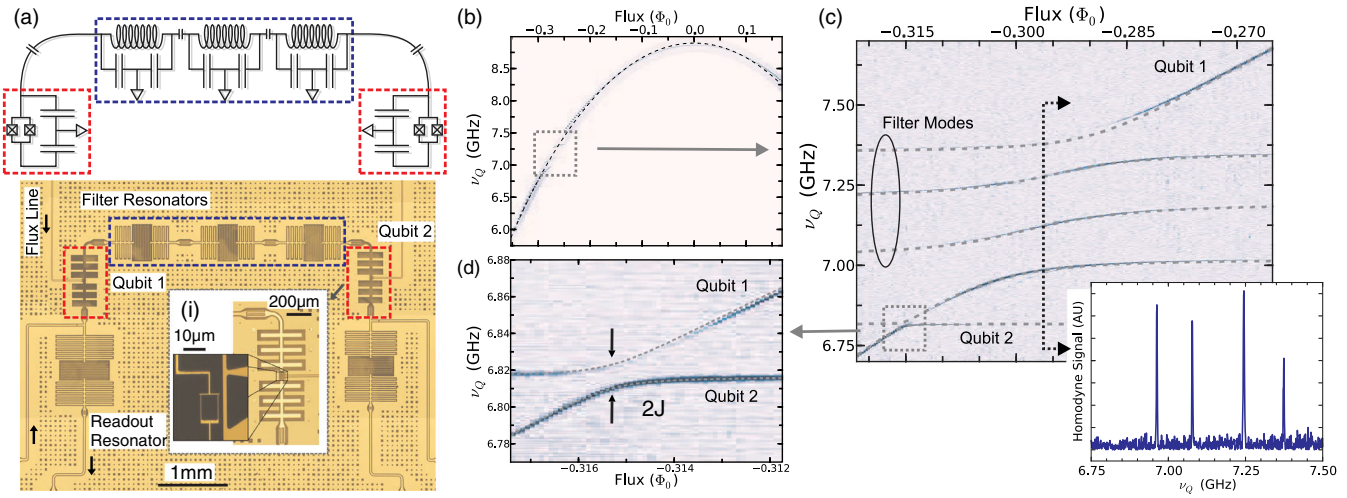

FIG. 1 (color online). Multimode device schematic and spectroscopy. (a) Schematic (top) and optical image (bottom) of our cQED device consisting of three lumped LC resonators (blue dotted line), which couple two transmon-type qubits (red dotted line). The qubits are coupled to readout resonators at $\nu_{1(2)} = 4.20(4.65)$ GHz. The qubit 1(qubit 2) lifetime $T_1 = 2.36(2.14)$ μs and the decay of Ramsey coherence (fit to Gaussian decay $e^{-t^2/2\sigma^2}$) is $\sigma = 312(492)$ ns. Full fabrication details, qubit properties, instrumentation, and cryogenic setup are given in Ref. [23]. (b) Single qubit spectroscopy as the qubit frequency ν_Q is tuned using the flux line. The dashed line is a fit obtained by diagonalizing the energy levels of the transmon in the charge basis. (c) Spectroscopy of the region where the qubit frequency crosses through the filter modes [dashed box in (b)]. The frequency of the other qubit is fixed and below the filter. The dashed lines are the eigenvalues of the Hamiltonian given by Eq. (1) using the qubit-filter parameters listed in the main text. The inset is a cross section of similar spectroscopy data demonstrating multimode strong coupling. (d) Spectroscopy of the qubit-qubit avoided crossing [dashed box in (c)]. In (b), (c), and (d) flux (in Φ_0) is obtained from experimental units as a fit parameter.

$$\hat{H} = \hat{H}_Q + \hat{H}_F + \hat{H}_{Q-F}, \tag{1}$$

$$\hat{H}_Q = h\nu_{Q,1}\hat{\sigma}_1^Z/2 + h\nu_{Q,2}\hat{\sigma}_2^Z/2, \tag{2}$$

$$\hat{H}_F = \sum_{i=1}^{n} h\nu_F \hat{a}_i^\dagger \hat{a}_i + \sum_{i=2}^{n} hg_F(\hat{a}_i^\dagger \hat{a}_{i-1} + \hat{a}_{i-1}^\dagger \hat{a}_i), \tag{3}$$

$$\hat{H}_{Q-F} = hg_{Q1,F}(\hat{a}_1^\dagger \hat{\sigma}_1^- + \hat{a}_1 \hat{\sigma}_1^+) + hg_{Q2,F}(\hat{a}_n^\dagger \hat{\sigma}_2^- + \hat{a}_n \hat{\sigma}_2^+), \tag{4}$$

where $\hat{a}_i^\dagger$ creates a photon in the ith resonator, $\hat{\sigma}^{+(-)}$ is the raising (lowering) operator for the qubit, $\hat{\sigma}^Z$ is the Pauli-Z operator, g_F is the filter-filter coupling, and $g_{Q,F}$ is the qubit-filter coupling.

Strong coupling between the bare filter resonators splits the three degenerate resonators into three "filter" modes with frequencies $\nu_1, \nu_2, \nu_3 = \nu_F - \sqrt{2}g_F, \nu_F, \nu_F + \sqrt{2}g_F$. Each of these filter modes is a superposition of photons in the bare resonators. Crucially, every filter mode has nonzero weight in the resonators at either end of the chain so that filter photons in mode i strongly couple to qubit 1 (qubit 2) with coupling $g_{Q1,Fi}(g_{Q2,Fi})$—this realizes our multimode strong coupling architecture. We fit the spectroscopy data in Fig. 1(c) to extract bare qubit-filter parameters $\nu_F = 7.169$ GHz, $g_F = 118$ MHz, and $g_{Q1,F}(g_{Q2,F}) = 135(144)$ MHz corresponding to multimode coupling parameters $g_{Q1,F2}(g_{Q2,F2}) = 95(102)$ MHz ($g_{Q,F1} = g_{Q,F3} = g_{Q,F2}/\sqrt{2}$).

When the qubits are detuned from all the filter modes and the filter is empty (analogous to the stop band of a classical filter) residual interactions are mediated by virtual photons through all modes and we can rewrite Eq. (1) as

$$\hat{H} = \hat{H}_Q + hJ(\hat{\sigma}_1^+ \otimes \hat{\sigma}_2^- + \hat{\sigma}_1^- \otimes \hat{\sigma}_2^+) + h\xi\hat{\sigma}_1^Z \otimes \hat{\sigma}_2^Z, \tag{5}$$

where J is the exchange term and ξ is the controlled-phase (c-phase) rate. If we consider identical qubit 1 and qubit 2 filter couplings g_Q and let Δ be the averaged detuning of the qubit from the bare filter mode (i.e., $\Delta = (\nu_{Q1} + \nu_{Q2} - 2\nu_F)/2$), then we can approximate J and ξ (for an n-mode filter) as

$$J \approx \frac{g_Q^2}{g_F}\left(\frac{g_F}{\Delta}\right)^n, \qquad \xi \approx \frac{4nJ^2}{\Delta}. \tag{6}$$

Notably, these rates are suppressed exponentially in the number of filter modes n, in terms of the small parameter g_F/Δ. To confirm the off-rate scaling predicted by Eq. (6), we directly measure the exchange term J from qubit spectroscopy, and numerically calculate the c-phase rate. The data plotted in Fig. 2 agree well with the model with no free parameters, demonstrating the essential scaling of the multimode off rate, and implying an off rate less than 10 kHz for a qubit-qubit detuning of 50 MHz.

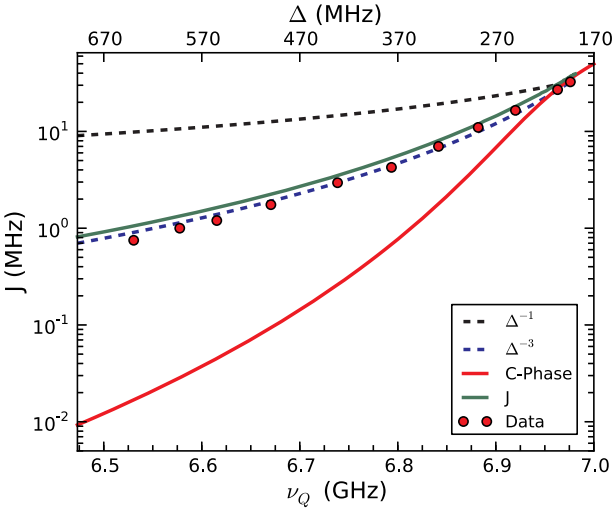

FIG. 2 (color online). Off-resonant coupling. Qubit-qubit exchange rate J as a function of the qubit frequency ν_Q (top axis, detuning Δ from the bare cavity frequency) for two different scaling laws (dashed lines), by numerical diagonalizing Eq. (1) (green line), and by measuring the exchange splitting (data points). We measure the exchange splitting from qubit spectroscopy, sample data is shown in Fig. 1(d). We also plot a numerical calculation of the c-phase rate [from Eq. (1)] versus the qubit 1 frequency using the filter parameters determined by the fit in Fig. 1 where qubit 2 is detuned below qubit 1 by 50 MHz (red line).

To enable strong interactions in the multimode architecture we tune the qubit frequency into resonance. In this limit, Eq. (6) is invalid, and the qubit interacts primarily with the closest mode with a coupling strength of order g_Q (the qubit-filter coupling). For our controlled-Z gate, we utilize these strong interactions by loading a real photon into the lowest filter mode and then employing a state-dependent one-photon Stark shift. Loading a single photon requires adiabatically traversing the qubit-filter avoided crossing shown in Fig. 1, so we first study the dynamics of this crossing by performing the experiment illustrated in Fig. 3(a). We excite qubit 1, raise the qubit energy quasilinearly through the filter in time t (the flux is ramped linearly), hold for time $T-2t$, ramp back in time t, and then measure the excited state population. Because we traverse avoided crossings twice, we observe interference fringes. Fast fringes, at short times, correspond to ramp speeds larger than the total filter bandwidth ($\gtrsim$400 MHz) where a significant fraction of the excitation remains with the qubit [31]. The slower fringes correspond to the excitation being distributed over multiple filter modes and the fringe frequency is fixed by the filter mode splitting. The multimode nature of the crossing is advantageous; although the ramp is not adiabatic with the lowest filter mode unless it is slower than $\approx$25 ns, the excitation remains in the filter for ramps $>$ 5 ns. We exploit this multimode Landau-Zener physics to transfer population to the filter faster than the single mode adiabatic limit.

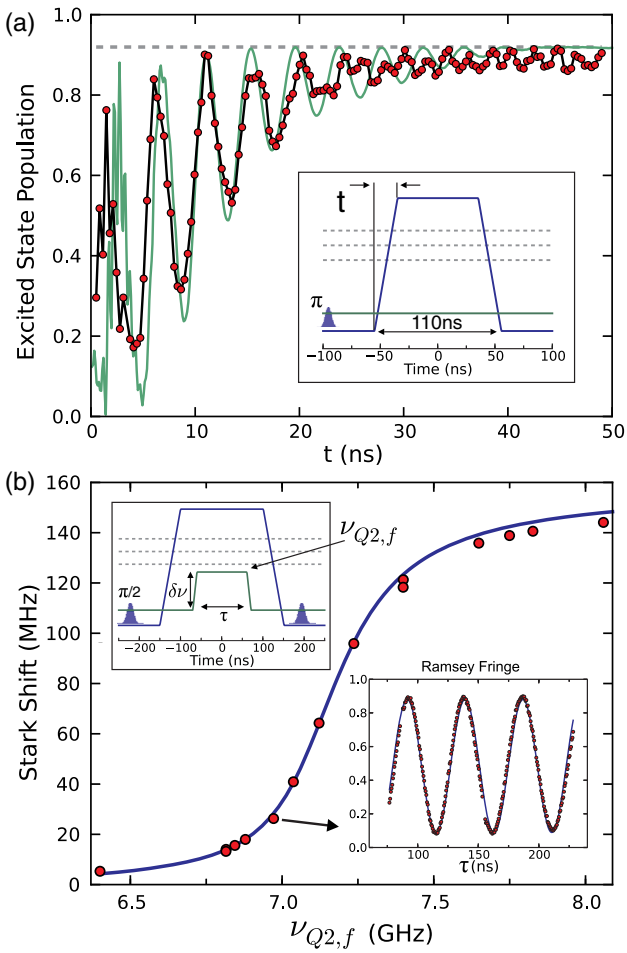

FIG. 3 (color online). Single photon loading and Stark shift. (a) To study the dynamics of loading single photons into the filter we traverse the qubit-filter avoided crossing in variable time t (protocol illustrated in inset and described in the main text). We plot the qubit excited state population versus the ramp time t: the solid black line is a guide to the eye, the dashed gray line is the expected maximum state population given T_1 decay, and the green solid line is a numerical solution of the Schrödinger equation using the Hamiltonian given by Eq. (1) and scaled by T_1 decay. (b) To measure the Stark shift between a single photon in the lowest mode of the filter and a qubit at bare frequency $\nu_{Q2,f}$ we perform a Ramsey experiment (protocol illustrated in inset and described in the main text). We plot the Stark shift as a function of $\nu_{Q2,f}$ and compare against a theory curve (blue solid line) with no free parameters. We use $\nu_{Q2,f} =$ 5.3 GHz as the reference height (i.e., set the Stark shift at that point to zero).

Next, we measure the Stark shift between a single photon and a qubit in the ground state by performing the Ramsey experiment illustrated by Fig. 3(b). First, we prepare qubit 1 in a superposition state and then raise the qubit frequency through the filter to create a photon superposition state. Next, we raise the frequency of qubit 2 to $\nu_{Q2,f}$ for a variable time τ. After a fixed total time, we retrieve the photon from the filter, apply a $\pi/2$ pulse, and measure the

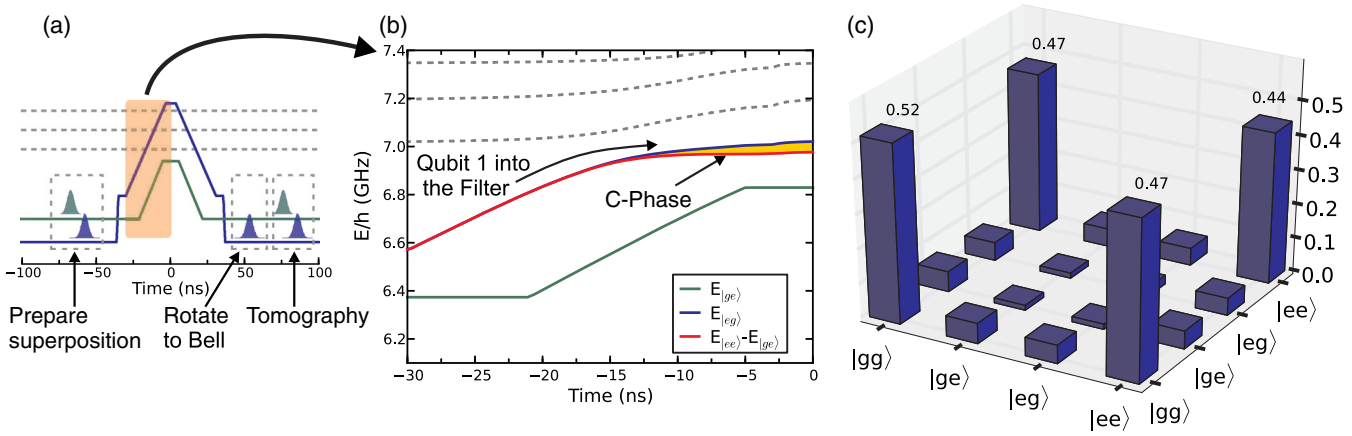

FIG. 4 (color online). Bell state and CZ gate. (a) Timing diagram for our Bell state experiment illustrating the flux pulses (solid lines) and microwave pulses (Gaussian). (b) The energy levels calculated from Eq. (1) in the orange region highlighted in (a). When qubit 1 crosses the filter, the qubit excitation is converted into a photon in the lowest filter mode. When qubit 2 is raised, the energy of the filter photon depends on the state of qubit 2, which generates a c phase; the total phase is the yellow area. (c) Absolute value of the density matrix elements after state tomography of the Bell state produced by the gate [23].

state of qubit 1. Because of the variable time interaction with qubit 2, we measure a Ramsey fringe versus τ. The frequency of the fringe is the Stark shift; sample data for one of the points are shown in the inset to Fig. 3(b). Approaching the filter from below, the Stark shift increases as $\approx 1/\Delta$, and then saturates at the maximum interaction (approximately the filter splitting $\sqrt{2}g_F = 167$ MHz) as qubit 2 is brought through the filter. The data agree very well with a theory curve with no free parameters, thus validating that we are loading a single photon into the lowest filter mode.

Finally, we combine the capabilities probed in the previous two experiments—loading a single photon into the filter and generating a strong Stark shift—to construct a quantum logic gate. The protocol for the gate is illustrated in Fig. 4(a). First, we convert the qubit 1 excitation into a photon, then we move qubit 2 close to the filter to acquire a state dependent Stark shift, and then we return the photon back to qubit 1. While the qubit energies cross during these ramps, we observe no evidence of an exchange process since our multimode filter strongly suppresses the off-resonance interaction [Eq. (6)]. We realize a controlled-Z (CZ) gate because the conditional phase $\phi_{c-\mathrm{phase}} = \phi_{|ee\rangle} + \phi_{|gg\rangle} - (\phi_{|eg\rangle} + \phi_{|ge\rangle})$ [calculated in Fig. 4(b)] is π. The full transmon-photon interaction exploited for this gate is discussed in Ref. [23]. The flux pulse sequence for our CZ gate is illustrated in Fig. 4. The total gate time, 95 ns, is optimized to maximize gate fidelity. For 50 MHz detuning between the qubits, this implies a gate contrast (on/off rate) greater than 1000 even for relatively small $\Delta/g_F \approx 5$.

To demonstrate the gate we prepare a Bell state, ideally $|\Psi_{\mathrm{Bell}}\rangle = (|gg\rangle + e^{i\Phi}|ee\rangle)/\sqrt{2}$. To characterize the density matrix we perform state tomography [32] on both qubits after the gate [see Fig. 4(c)]. The fidelity $F = \langle\Psi_{\mathrm{Bell}}|\rho_{\mathrm{meas}}|\Psi_{\mathrm{Bell}}\rangle$ is $0.947 \pm 0.005_{\mathrm{stat}} \pm 0.01_{\mathrm{sys}}$ corresponding to a concurrence of $0.926 \pm 0.01_{\mathrm{stat}} \pm 0.02_{\mathrm{sys}}$ [33]. We also measure a full process fidelity of 0.89 [23]. Our fidelity is comparable to other contemporary results (two-qubit entangled states have been produced with state fidelities up to 99.5% [12] and a concurrence of 0.994 [34]), and a master equation simulation of the gate [23] suggests that our fidelity is limited by lifetime, rather than the protocol. One advantage of our protocol is that our gate is relatively insensitive to inhomogeneous broadening due to flux noise; once the qubit excitation is a photon in the filter, the energy is not flux dependent. Several improvements are possible, for example, engineering a flux insensitive bias point below the filter for state preparation [35], utilizing new materials [36], and material processing for high Q resonators [37], as well as reducing the total gate time using techniques from optimal control for crossing the filter.

In conclusion, we have demonstrated a new multimode architecture for coupling superconducting qubits. We measured that the off-resonance coupling is suppressed exponentially in the number of modes, while still maintaining strong interactions when the qubits are tuned close to resonance. We used these capabilities to realize a high-contrast controlled-Z gate. Further, this work indicates a need to develop a microwave filter theory for coherent quantum systems. The multimode architecture is a promising platform for realizing lattice based quantum simulations and photonic registers for quantum information processing.

We acknowledge support from the University of Chicago MRSEC, the Army Research Office under Grant No. W911NF-12-1-0608, the Alfred P. Sloan Foundation, the NSF under Grant No. DMR-1151839, and the DARPA under Grant No. N66001-11-1-4123. We

acknowledge David Czaplewski at the Argonne Center for Nanomaterials for assistance with the optical lithography. We thank J. Chow and B. Johnson for discussions and J. Thywissen for manuscript comments.

*dcmckay@uchicago.edu
†Present address: Yale Department of Applied Physics, New Haven, Connecticut 06511, USA.

[1] M. Devoret and R. Schoelkopf, Science **339**, 1169 (2013).
[2] A. A. Houck, J. A. Schreier, B. R. Johnson, J. M. Chow, J. Koch, J. M. Gambetta, D. I. Schuster, L. Frunzio, M. H. Devoret, S. M. Girvin *et al.*, Phys. Rev. Lett. **101**, 080502 (2008).
[3] S. E. Nigg, H. Paik, B. Vlastakis, G. Kirchmair, S. Shankar, L. Frunzio, M. H. Devoret, R. J. Schoelkopf, and S. M. Girvin, Phys. Rev. Lett. **108**, 240502 (2012).
[4] D. J. Egger and F. K. Wilhelm, Phys. Rev. Lett. **111**, 163601 (2013).
[5] L. Zhou, H. Dong, Y.-X. Liu, C. P. Sun, and F. Nori, Phys. Rev. A **78**, 063827 (2008).
[6] S. Schmidt and J. Koch, Ann. Phys. (Amsterdam) **525**, 395 (2013).
[7] M. Mariantoni, H. Wang, T. Yamamoto, M. Neeley, R. C. Bialczak, Y. Chen, M. Lenander, E. Lucero, A. D. OConnell, D. Sank *et al.*, Science **334**, 61 (2011).
[8] M. D. Reed, B. R. Johnson, A. A. Houck, L. DiCarlo, J. M. Chow, D. I. Schuster, L. Frunzio, and R. J. Schoelkopf, Appl. Phys. Lett. **96**, 203110 (2010).
[9] E. Jeffrey, D. Sank, J. Mutus, T. White, J. Kelly, R. Barends, Y. Chen, Z. Chen, B. Chiaro, A. Dunsworth *et al.*, Phys. Rev. Lett. **112**, 190504 (2014).
[10] C. Rigetti, J. M. Gambetta, S. Poletto, B. L. T. Plourde, J. M. Chow, A. D. Córcoles, J. A. Smolin, S. T. Merkel, J. R. Rozen, G. A. Keefe *et al.*, Phys. Rev. B **86**, 100506 (2012).
[11] S. Gustavsson, O. Zwier, J. Bylander, F. Yan, F. Yoshihara, Y. Nakamura, T. P. Orlando, and W. D. Oliver, Phys. Rev. Lett. **110**, 040502 (2013).
[12] R. Barends, J. Kelly, A. Megrant, A. Veitia, D. Sank, E. Jeffrey, T. C. White, J. Mutus, A. G. Fowler, B. Campbell *et al.*, Nature (London) **508**, 500 (2014).
[13] L. DiCarlo, M. D. Reed, L. Sun, B. R. Johnson, J. M. Chow, J. M. Gambetta, L. Frunzio, S. M. Girvin, M. H. Devoret, and R. J. Schoelkopf, Nature (London) **467**, 574 (2010).
[14] A. Fedorov, L. Steffen, M. Baur, M. da Silva, and A. Wallraff, Nature (London) **481**, 170 (2012).
[15] J. M. Chow, J. M. Gambetta, E. Magesan, D. W. Abraham, A. W. Cross, B. R. Johnson, N. A. Masluk, C. A. Ryan, J. A. Smolin, S. J. Srinivasan *et al.*, Nat. Commun. **5**, 4015 (2014).
[16] O.-P. Saira, J. P. Groen, J. Cramer, M. Meretska, G. de Lange, and L. DiCarlo, Phys. Rev. Lett. **112**, 070502 (2014).
[17] R. Schutjens, F. A. Dagga, D. J. Egger, and F. K. Wilhelm, Phys. Rev. A **88**, 052330 (2013).
[18] S. J. Srinivasan, A. J. Hoffman, J. M. Gambetta, and A. A. Houck, Phys. Rev. Lett. **106**, 083601 (2011).
[19] R. C. Bialczak, M. Ansmann, M. Hofheinz, M. Lenander, E. Lucero, M. Neeley, A. D. OConnell, D. Sank, H. Wang, M. Weides *et al.*, Phys. Rev. Lett. **106**, 060501 (2011).
[20] Y. Chen, C. Neill, P. Roushan, N. Leung, M. Fang, R. Barends, J. Kelly, B. Campbell, Z. Chen, B. Chiaro *et al.*, Phys. Rev. Lett. **113**, 220502 (2014).
[21] M. S. Allman, J. D. Whittaker, M. Castellanos-Beltran, K. Cicak, F. da Silva, M. P. DeFeo, F. Lecocq, A. Sirois, J. D. Teufel, J. Aumentado *et al.*, Phys. Rev. Lett. **112**, 123601 (2014).
[22] J. Koch, T. M. Yu, J. Gambetta, A. A. Houck, D. I. Schuster, J. Majer, A. Blais, M. H. Devoret, S. M. Girvin, and R. J. Schoelkopf, Phys. Rev. A **76**, 042319 (2007).
[23] See Supplemental Material at http://link.aps.org/supplemental/10.1103/PhysRevLett.114.080501, which includes Refs. [22,24–30,32], for an expanded theoretical discussion (e.g., a derivation of Eq. 6) and further experimental details (e.g., sample fabrication and calibrations).
[24] D. Sank, R. Barends, R. C. Bialczak, Y. Chen, J. Kelly, M. Lenander, E. Lucero, M. Mariantoni, A. Megrant, M. Neeley *et al.*, Phys. Rev. Lett. **109**, 067001 (2012).
[25] B. Johnson, Ph.D. thesis, Yale University, 2010.
[26] J. M. Chow, L. DiCarlo, J. M. Gambetta, F. Motzoi, L. Frunzio, S. M. Girvin, and R. J. Schoelkopf, Phys. Rev. A **82**, 040305(R) (2010).
[27] J. M. Chow, L. DiCarlo, J. M. Gambetta, A. Nunnenkamp, L. S. Bishop, L. Frunzio, M. H. Devoret, S. M. Girvin, and R. J. Schoelkopf, Phys. Rev. A **81**, 062325 (2010).
[28] M. A. Nielsen and I. L. Chuang, *Quantum Computation and Quantum Information* (Cambridge University Press, Cambridge, England, 2000).
[29] J. L. O'Brien, G. J. Pryde, A. Gilchrist, D. F. V. James, N. K. Langford, T. C. Ralph, and A. G. White, Phys. Rev. Lett. **93**, 080502 (2004).
[30] T. Yamamoto, M. Neeley, E. Lucero, R. C. Bialczak, J. Kelly, M. Lenander, M. Mariantoni, A. D. OConnell, D. Sank, H. Wang *et al.*, Phys. Rev. B **82**, 184515 (2010).
[31] Y. Kayanuma and S. Fukuchii, J. Phys. B **18**, 4089 (1985).
[32] D. F. V. James, P. G. Kwiat, W. J. Munro, and A. G. White, Phys. Rev. A **64**, 052312 (2001).
[33] W. K. Wootters, Phys. Rev. Lett. **80**, 2245 (1998).
[34] J. M. Chow, J. M. Gambetta, A. D. Córcoles, S. T. Merkel, J. A. Smolin, C. Rigetti, S. Poletto, G. A. Keefe, M. B. Rothwell, J. R. Rozen *et al.*, Phys. Rev. Lett. **109**, 060501 (2012).
[35] J. D. Strand, M. Ware, F. Beaudoin, T. A. Ohki, B. R. Johnson, A. Blais, and B. L. T. Plourde, Phys. Rev. B **87**, 220505(R) (2013).
[36] J. B. Chang, M. R. Vissers, A. D. Crcoles, M. Sandberg, J. Gao, D. W. Abraham, J. M. Chow, J. M. Gambetta, M. B. Rothwell, G. A. Keefe *et al.*, Appl. Phys. Lett. **103**, 012602 (2013).
[37] A. Megrant, C. Neill, R. Barends, B. Chiaro, Y. Chen, L. Feigl, J. Kelly, E. Lucero, M. Mariantoni, P. J. J. OMalley *et al.*, Appl. Phys. Lett. **100**, 113510 (2012).